Journal of Asian Concrete Federation
Vol. 9, No. 1, pp. 43-50, June 2023
ISSN 2465-7964 / eISSN 2465-7972
DOI http://dx.doi.org/10.18702/acf.2023.9.1.43

Technical Paper

Investigation of the filling-overflow behavior of corrosion products in reinforced mortar

Dandan Xu, Yuzhou Wang, Haiyu Wang, Yuxi Zhao*

(Received April 05, 2023; Revised April 21, 2023; Accepted May 06, 2023; Published June 30, 2023)

Abstract: The investigation of the filling-overflow behavior of corrosion products in concrete is important for accurately predicting corrosion-induced concrete cover cracking. This paper utilizes the ethylene diamine tetra acetic acid (EDTA) titration method to quantitatively study the iron content in each zone of corroded reinforced mortar specimens. Based on this, the proportion and distribution of corrosion products are analyzed. Results show that approximately 50% of the corrosion products are transported to the mortar and corrosion products show a transport pattern to the surrounding low-concentration area in mortar. The direction of ion invasion on the mortar specimen does not exhibit a significant impact on the transport of corrosion products, while both the geometric size and quality of the mortar specimen affect the transport of corrosion products. Furthermore, the proposed method employs EDTA titration to quantify the filling and overflow of corrosion products, providing a valuable approach for further experimental research.

Keywords: Durability; Steel corrosion; Corrosion products; EDTA titration method.

1. Introduction

Steel corrosion is a primary cause of the deterioration of reinforced concrete structures. The corrosion products generated by steel corrosion can accumulate at the steel-concrete interface and produces corrosion-induced expansion pressure on the concrete, eventually leading to concrete cracking and accelerated structural deterioration. However, part of the corrosion products is transported into the concrete and does not accumulate at the steel-concrete interface, which was demonstrated by both engineering practice and academic research. This transport behavior inherently refers to the fact that ferrous ions that are released at the steel surface during the corrosion process transport away from the steel in the concrete pore solution [1].

Studies on the collapse of the Ynys-y-Gwas bridge in the UK by Woodward and Williams [2] found that the prestressing tendons were severely corroded at the joints, leading to fracture. However, the bridge did not show signs of significant degradation such as cracking and spalling, indicating that the proportion of corrosion products causing corrosion expansion effects was minimal. Additionally, Pape and Melchers [3] investigated a 45-year-old prestressed bridge girder section in Australia and showed that some of the corrosion products did not adhere to the surface of the rebar but filled in areas away from the steel-concrete interface. Melchers and Li [4] and Cavalier [5] found severe localized corrosion of the rebar in their investigation, but no corrosion products with the volume corresponding to the volume of steel loss were found in the concrete near the severely corroded section. This suggests that some of the corrosion products are transported away from the rebar and may be lost to the environment. The findings underscore the importance of considering the possibility that corrosion products can stay in other locations in concrete away from the steel-concrete interface or even be lost to the external environment.

Scholars have carried out extensive studies on the filling behavior of corrosion products in concrete and established relevant models. Some studies have proposed concepts such as "porous zone" [6,7] and "corrosion accommodating region (CAR)" [8] to describe the limited filling range of corrosion products in concrete. The filling range of corrosion products has been measured by subsequent studies

***Corresponding author Yuxi Zhao** *is a Professor at College of Civil Engineering and Architecture, Zhejiang University, Hangzhou, PR China.*

Dandan Xu *is a Ph.D. student at College of Civil Engineering and Architecture, Zhejiang University, Hangzhou, PR China.*

Yuzhou Wang *is a Doctor of Engineering at College of Civil Engineering and Architecture, Zhejiang University, Hangzhou, PR China.*

Haiyu Wang *is a Master of Engineering at College of Civil Engineering and Architecture, Zhejiang University, Hangzhou, PR China.*

and found to be in the range of tens to hundreds of micrometers. Empirical relationships between the thickness of corrosion product-filled paste (CP) and corrosion layer (CL) have been established based on a large number of test data [9-11]. It was observed that the thickness of CP exhibits a positive correlation with the thickness of CL, albeit with a diminishing growth rate that culminates in a state of stabilization. Dong [12] conducted tests and proposed that the maximum value of CP thickness increases with time, speculating that when a concrete structure is in service in an exposed environment for a long period enough period of time, the CP range may include the entire concrete cover, after which the corrosion products may be lost from the concrete. However, this hypothesis is yet to be proven by test results. Wang [13] further classified corrosion products into three categories: corrosion layer (CL), corrosion products filling into concrete (FCP), and overflowed corrosion products (OCP), and proposed the filling-overflow coefficient KT ((FCP+OCP)/CL) to clarify the ratio between corrosion products that do not cause corrosion expansion and those that do. However, further research is still needed to understand the influence of filling-overflow behavior by material parameters and the distribution pattern of FCP in mortar.

This paper focuses on the filling-overflow behavior of corrosion products in mortar specimens. And the total amount of filled and overflowed corrosion products is defined as the transported corrosion products (TCP). For the quantitative calculation of different types of corrosion products, existing methods include the measurement of CP and CL thicknesses using the scanning electron microscope (SEM) and the indirect calculation of KT (TCP/CL) based on the extraction of corrosion layer area and cross-sectional loss rate from XCT images. However, the method proposed in this paper is for the first time to quantitatively determine the distribution of the amount of TCP in the mortar using EDTA titration.

The objective of this work is to investigate the proportion and distribution of different types of corrosion products in mortar using EDTA titration tests. To achieve this goal, four types of reinforced mortar specimens with different water-cement ratios and cover thicknesses were studied. After 23-month exposure to chloride-rich environments, the specimens were processed into different small concrete blocks. Then, the corroded steel bar and the steel-mortar interface were acid-washed and the mass of iron in the corrosion layer was quantified by the acid-washing solution, while the distribution of the mass of iron in the mortar was determined by drilling and titrating the powder samples drilled from different zones. This study will contribute to a better understanding of the filling-overflow process of corrosion products in mortar and the related influencing factors.

2. Experimental program

2.1 Specimens

To minimize the interference of iron content in both aggregate and cement, we cast mortar blocks using reference cement and standard sand. These materials were chosen because their original iron content could be determined when the casting ratio is determined. The chemical composition of reference cement and standard sand are shown in Table 1 and Table 2, respectively. Meanwhile, deionized water instead of tap water was used for casting to avoid the interference of iron from the outside world. The 3-day compressive strength of the mortar blocks, as determined by testing, was 28.1 MPa. Each specimen contains a 20 mm diameter HRB335 rebar, and the chemical composition of the bar is shown in Table 3.

Our test consisted of four mortar specimens, which were numbered MR-c, where M represents the mortar specimen, R denotes the water-cement ratio, and c indicates the cover thickness. Table 4 summarizes the mortar mix design, the mass of rebar, and the dimension of mortar specimens.

A mortar specimen with the dimensions is shown in Figure 1. To avoid interference from end corrosion, the rebar ends were wrapped with epoxy resin, and the five faces of the specimen were coated with the epoxy resin as well. This coating ensured that the mortar specimen is in a state where chloride ions can only invade from the top surface, and that the direction of water diffusion and evaporation was controlled.

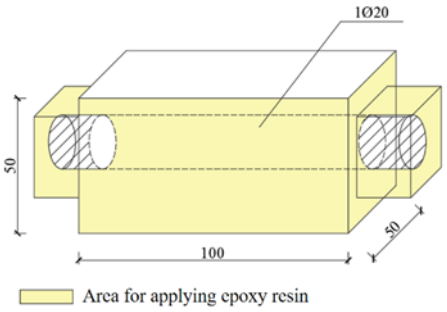

Fig. 1: Schematic diagram of the reinforced mortar specimen (dimensions in mm).

Table - 1. Chemical composition of reference cement

Composition	SiO_2	Al_2O_3	Fe_2O_3	CaO	MgO	SO_3	R_2O	f-CaO	Loss	Cl^-
Proportion(%)	20.94	4.85	3.44	64.02	1.70	1.88	0.50	0.50	1.88	0.011

Table - 2. Chemical composition of ISO standard sand

Composition	SiO_2	Al_2O_3	Fe_2O_3	CaO	MgO	Loss
Proportion(%)	98.50	0.83	0.07	0.12	0.11	0.24

Table - 3. Chemical composition of rebar

Composition	Fe	Mn	Si	S	P	Cu	Ni	Mo
Proportion(%)	98.00	1.10	0.72	0.01	0.02	0.08	0.06	/

Table - 4. The labels of the four specimens in the study

Specimen number	Mixture proportions(kg/m^3)				Mass of rebar (g)	Specimen dimension (mm)
	Cement	Fine aggregates	Deionized water	Chloride ion content		
M0.5-10	450	1350	225	9	302.0	40*40*100
M0.5-15	450	1350	225	9	286.1	50*50*100
M0.5-20	450	1350	225	9	301.6	60*60*100
M0.65-15	450	1350	292.5	9	291.2	50*50*100

2.2 Curing and exposure history

Following a curing period of 28 days, the specimens were individually placed in sealed polyethylene boxes to initiate accelerated corrosion through wetting and drying cycles. The wetting cycle involved immersing the specimens in a 3.5% NaCl solution which was prepared using deionized water, and this process lasted for 24 hours. Subsequently, the specimens were removed from the solution and placed in a separate polyethylene box. This box was then placed in a chamber with constant temperature and humidity (25℃ and 50% relative humidity) for drying, which lasted for 72 hours. The specimens underwent a total of 18 months of wetting and drying cycles, following which they were placed in a 3.5% NaCl solution for five months.

2.3 Sample preparation

2.3.1 Specimen cutting

The specimens were removed and placed in a polyethylene box in a constant temperature and humidity chamber to dry for 7 days, and then cutting was started. Firstly, the mortar specimen was cut along the red dotted line parallel to the length direction, then rebar was removed, and the mortar specimen was divided into two half blocks, the one containing the exposed surface being labelled as A, and the other as B. The steel/mortar interface and the corroded rebar were acid-washed after coating 20 mm of the rebar ends and 10 mm of the mortar block ends with epoxy resin.

The acid washing solution was prepared following the specification Standard Practice for Preparing, Cleaning, and Evaluating Corrosion Test Specimens (ASTM G1-90:1999 [14]). For the acid washing of the steel/mortar interface, visible corrosion products adhering to the interface were scraped off with a copper carving knife first. Then, a brush soaked in the acid washing solution was used to clean the interface until no rust residue was visible to the naked eye. The residual acid washing solution in the sponge was rinsed with deionized water and added to the solution for testing. The resulting solution was then filtered using a vacuum filter to remove any precipitate, and finally was collected and stored for subsequent titration, named " MR-c -L". After acid washing, the mass of the rebar was recorded.

Using a precision cutting machine (SYJ-200), half mortar block was cut into three small blocks, after removing the 10 mm thickness of the specimen at both ends. The small blocks were then divided into rectangular standard zones measuring 10 mm x 5 mm in cross-section. Powder samples for testing were extracted from these zones using a handheld drill with a 5 mm chrome vanadium drill bit. The powder samples were named using a row number and column number format. Since the cross-section of the small block is symmetrical and the boundary conditions were basically the same, the powder samples taken from the symmetrical zones were combined and named using the smaller number. For example, in Figure 2, powder sample 11 of A1 is combined with sample 15 and named 11. If the zone around the rebar is smaller than a standard one, it was

combined with the adjacent zone that had similar conditions, such as sample 42 and sample 52 were combined and named 42.

2.3.2 Weight loss method

The acid washing solution was prepared following the specification Standard Practice for Preparing, Cleaning, and Evaluating Corrosion Test Specimens (ASTM G1-90:1999 [14]). In addition to the corroded rebar, the same method was used for an uncorroded one of the same type, and the resulting acid washing solution was collected and labelled as L0. Afterward, L0 was titrated to calibrate the amount of steel loss on the rebar due to the acid-acid washing process. After drying the bars, the remaining mass was measured and recorded to calculate the corrosion rate using the following equation.

$$\rho = \frac{(m_0 - m_r) - (m_{0r} - m_{rr})}{m_0} \quad (1)$$

Where m_0 is the original mass of the corroded rebar (g), m_r is the residual mass of the corroded one after acid washing(g), m_{0r} is the original mass of the reference one (g), m_{rr} is the residual mass of the reference one after acid washing (g).

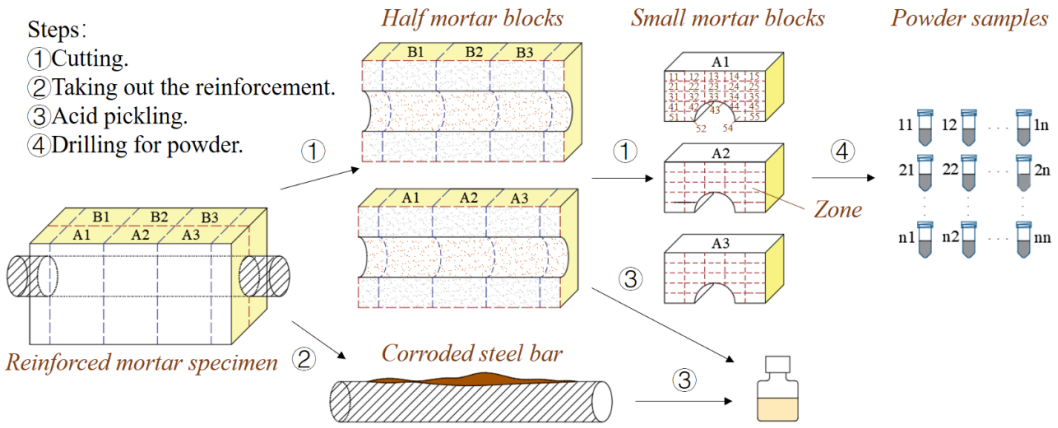

Fig. 2: Sample preparation.

Table - 5. Corrosion-induced mass loss of steel.

Specimen number	Original mass (g)	Mass after acid washing (g)	Mass loss (g)	Corrosion rate (%)
M0.5-10	302.0	300.5	1.5	0.50
M0.5-15	286.0	284.9	1.1	0.38
M0.5-20	301.6	300.8	0.8	0.23
M0.65-15	291.0	288.1	2.9	1.00

Table - 6. Titration results of the acid washing solution of the corrosion layer.

Specimen number	Total volume of acid washing solution (ml)	Volume of participating titration (ml)	Average value of EDTA consumption (ml)	Total mass of Fe^{3+} (g)
M0.5-10-L	261.3	2.5	27.55	0.80
M0.5-15-L	258.3	2.5	22.21	0.64
M0.5-20-L	368.4	2.5	10.42	0.43
M0.65-15-L	630.1	2.5	19.19	1.35

2.3.3 EDTA titration tests

The determination of iron content in mortar was carried out by EDTA titration test, according to Chinese specification GB/T 176-2017 [15]. Before titration, mortar powder samples underwent pretreatment, and the titration result was averaged over three samples from the same zone.

The molar mass of iron used in this paper is 55.847 and the mass of iron in the sample to be measured is calculated as follows.

$$m_{Fe} = c_{EDTA} \times V_{EDTA} \times 55.847 \times 10 \quad (2)$$

Where m_{Fe} is the mass of iron (g), c_{EDTA} is the molar concentration of EDTA standard solution (mol/L), V_{EDTA} is the volume of EDTA solution consumed for titration (mL). And 10 represents the volume ratio of the total specimen solution to the specimen solution taken.

3. Results and discussion

3.1 Corrosion of rebar

The corroded rebar was removed from the mortar specimen and a reddish-brown corrosion layer was evident on the surface. The mass of the rebar before corroding and after acid washing, and the corrosion rate are shown in Table 5 below.

It can be found that with the increase of the cover thickness, the mass loss and corrosion rate of corroded rebar decrease continuously. Moreover, the corrosion rate of the rebar in the mortar specimen with a water-cement ratio of 0.65 is much larger than that of the specimen with a water-cement ratio of 0.5. The results show that the quality of mortar has a greater effect on the corrosion rate, which should be strictly controlled in the actual project.

3.2 Corrosion layer analysis

The reddish-brown corrosion products were found to adhere to the interface at the steel/mortar interface, and the phenomenon of more corrosion products on the side near the exposed surface than on the side away from the exposed surface was observed. Additionally, for the higher water-cement ratio specimens, the amount of corrosion products appears significantly more on both sides.

It can be attributed to the fact that the mortar is in a state where chloride ions can only invade from the top surface. As a result, the rebar is more accessible to moisture and oxygen on the side near the exposed surface, leading to the formation of more corrosion micro-cells on the surface, which becomes the corrosion anode, while the other side becomes the corrosion cathode, promoting the corrosion. And specimens with a higher water-cement ratio have poor mortar quality and be more susceptible to corrosion.

The corrosion layer is collected from the steel bar surface and the steel-mortar interface. The titration results (0.005 mol/L EDTA standard solution) of the acid washing solution of the corrosion layer are shown in Table 6.

3.3 Analysis of the transported corrosion products (TCP)

3.3.1 Analysis of the proportion of TCP

The difference between the mass loss of the rebar and the iron mass forming the corrosion layer is the iron mass corresponding to TCP. Despite the accuracy of the rebar mass weighing being 0.1g, the error associated with the determination of TCP's iron mass is insignificant and does not alter the general trend.

The proportion of the iron mass of CL and TCP to total corrosion products is shown in Figure 3, respectively. The transport proportion for three specimens with the same water-cement ratio of 0.5 is similar, suggesting that the cover thickness has no impact on the transport of corrosion products. However, the transport portion of specimen M0.65-15 accounts for 53%, which is a significant increase compared with the other three, indicating that a higher water-cement ratio facilitates the outward transport of the corrosion products.

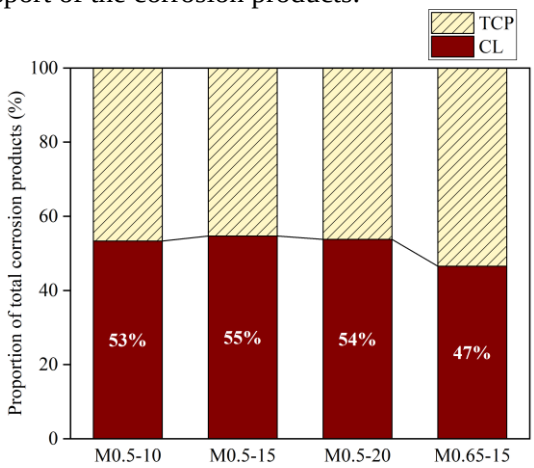

Fig. 3: The proportion of the iron mass of CL and TCP to total corrosion products.

3.3.2 Distribution pattern of FCP

The samples were prepared according to the procedure presented in Figure 2, and the powder samples were obtained by drilling from three small test blocks, A1, A2 and A3, where the iron content of each zone was determined by the EDTA titration method.

It is noteworthy that the iron content of the powder samples measured in the test includes the iron-containing compounds of the original mortar, which should be subtracted, and the initial iron content in the mortar can be calculated as follows.

$$\omega_{m,Fe} = \frac{(m_c \times \omega_{c,Fe_2O_3} + m_s \times \omega_{s,Fe_2O_3})}{m_m} \times \frac{M_{Fe} \times 2}{M_{Fe_2O_3}} \quad (3)$$

Where $\omega_{m,Fe}$ is the initial iron content in mortar, m_c and m_s are the mass of cement and that standard sand used at casting (g), m_m is the mass of mortar specimen (g), ω_{c,Fe_2O_3} and ω_{s,Fe_2O_3} are the iron content in cement and in standard sand, M_{Fe} and $M_{Fe_2O_3}$ are the relative atomic mass of Fe and Fe_2O_3, respectively. The theoretical initial iron content of the mortar specimen with a water-cement ratio of 0.5 was calculated to be 0.56%, and that with a water-cement ratio of 0.65 was 0.55%.

However, the homogeneity of mortar, that is, the non-uniformly distributed mortar and sand will cause fluctuation of local iron content. Therefore, to minimize the bias caused by the material nature, the

iron content in each zone was averaged over the data of three test samples, which were extracted from the same depth of the mortar cover. Then, by subtracting the initial iron content in original mortar, the increment of iron content contributed by corrosion products is shown in Figure 4.

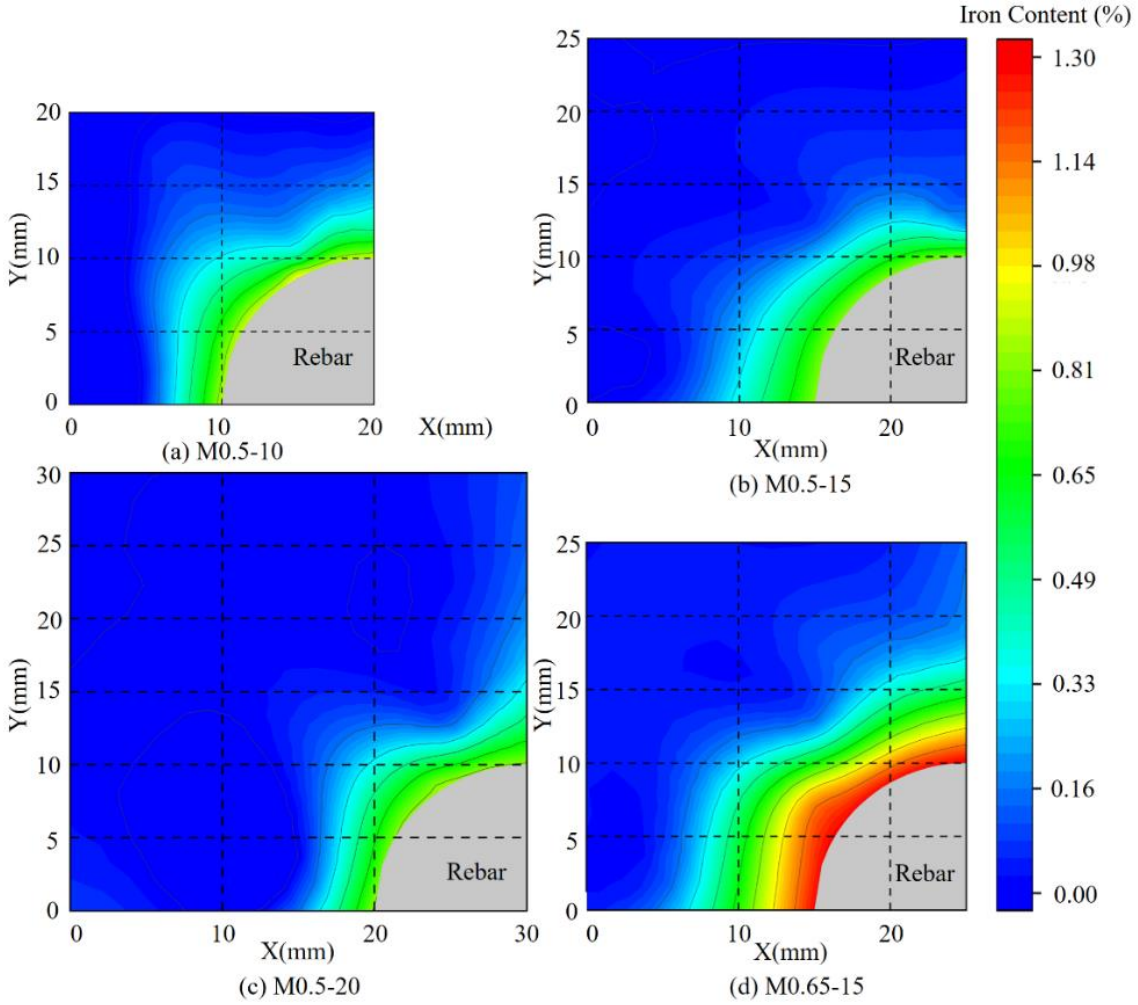

Fig. 4: The incremental iron content of each zone in mortar specimens.

The distribution of incremental iron content (relative to the original iron content of the mortar) in different zones within each small block was shown in Figure 4, reflecting the distribution of TCP. The image area drawn is a square with the center of the rebar as the bottom right vertex and the vertical distance to the exposed surface as the image side length (Y-axis direction). Due to the limitations of the test design, an interpolation method was employed to expand the data, and the iron content of the rebar surface was set to the maximum iron content of all test points to obtain an image that aligns more closely with the actual condition. Actually, this test design needs improvement since the powder extraction operation determined that the zone should not be too small, leading to fewer sampling points (especially in the horizontal direction), which limits the acquisition of more detailed results to reflect the overall pattern.

The titration results for the three specimens with a water-cement ratio of 0.5 were relatively close and had small standard deviations, except for several zones closest to the rebar. This implies that under the test conditions, in the specimen with a water-cement ratio of 0.5, the outward transport range of corrosion products is relatively limited, and the change of cover thickness has no obvious influence on it. By comparing the differences in the iron content in each zone of the M0.5-15 and M0.65-15, it can be verified that the transport range of corrosion products within the specimen M0.65-15 reaches the entire cross-section, indicating that the quality of mortar significantly affects the transport of corrosion products.

Furthermore, the iron content in the mortar section is the highest around the rebar and gradually decreases outward. Under the test conditions, no significant difference was found in the iron content distribution at the corresponding zones in the direction of the exposed and non-exposed surfaces. And Figure 4 shows that the iron content around the rebar is evenly distributed in the ring direction. Hence, it can be concluded that in the transport process of corrosion products to mortar, the

geometric size of the mortar specimen and the direction of chloride ion invasion are not the primary factors affecting the filling behavior, but the quality of mortar affects the filling behavior and the distribution of corrosion products within the mortar.

3.4 Over-flowed corrosion products analysis

Determining the existence of OCP, which overflow from the mortar into the external environment is an important issue focused on in this study. The phenomenon of corrosion products transport towards the specimen surface is evident in Figure 4. Notably, the transport phenomenon becomes more pronounced with an increasing water-cement ratio. This can be attributed to the increased porosity and apparent diffusion coefficient of ions in mortar [16,17], which facilitate the transport of corrosion products in the forms of ions.

Wang [13] utilized the same batch of specimens (M0.5-10, M0.5-15, and M0.5-20) with identical mix ratios and corrosion histories as in the present study, and make sure each wetting cycle was conducted in the same sealed box. After corrosion, the surface damage of each specimen was examined, and no crack formation was observed. Subsequently, 5 mL water samples of three specimens were extracted from the solution for immersion using a pipette and analyzed using a HORIBA laser confocal Raman spectrometer. In the water sample of specimen M-0.5-10, Raman characteristic peaks were detected in the characteristic peak interval 318~320 cm^{-1}(Fe^{3+}-Cl^{-}), whereas no significant characteristic peaks were detected in the other two water samples.

The test results indicate that after 18 months of drying and wetting cycles with a 3.5% NaCl solution, the corrosion products generated by the depassivation of the rebar in specimen M0.5-10 were transported to the external environment outside the specimen. This finding suggests that the transport range of corrosion products in the mortar specimen was at least 10 mm under the test condition. The corrosion products in specimens M0.5-15 and M0.5-20 have not yet been transported outside the specimen, indicating that the transport range is between 10 and 15 mm. This confirms the existence of OCP and highlights the influence of the cover thickness on the transport range of corrosion products.

4. Conclusions

1. The proposed method employs EDTA titration to quantify the filling and overflow of corrosion products, providing a valuable approach for further experimental research.
2. Nearly 50% of the corrosion products are transported to the mortar. The direction of ion invasion on the mortar specimen does not exhibit a significant impact on the transport of corrosion products. However, both the geometric size and quality of the mortar specimen have an effect on the transport of corrosion products.
3. In the half mortar block near the exposed surface, the corrosion products are relatively evenly spread around the rebar in the mortar, and show a transport pattern to the surrounding low-concentration zone in the radial direction.

Acknowledgments

Financial support from the National Natural Science Foundation of China (51978604) is gratefully acknowledged.

References

[1] Stefanoni, M.; Zhang, Z.; Angst, U. M.; & Elsener; B. (2018)“The kinetic competition between transport and oxidation of ferrous ions governs precipitation of corrosion products in carbonated concrete,” RILEM Technical Letters, 3, pp. 8-16.

[2] Woodward, R. J.; Williams, F. W. (1998). “Collapse of Ynys-y-Gwas bridge,” GLAMORGAN. Proceedings of the Institution of Civil Engineers, 84(4), pp. 635-669, Wales, UK.

[3] Pape, T. M.; Melchers, R. E. (2011) “The effects of corrosion on 45-year-old pre-stressed concrete bridge beams,” Structure and Infrastructure Engineering, 7, pp. 101-108.

[4] Melchers, R. E.; & Li, C. (2009) “Reinforcement Corrosion in Concrete Exposed to the North Sea for More than 60 Years,” Corrosion, 65, pp. 554-566.

[5] Cavalier, P.; Vassie, P. R.; & Trrl. (1981) “Investigation and repair of reinforcement corrosion in a bridge deck” Proceedings of the Institution of Civil Engineers, 70, pp. 461-480.

[6] Liu, Y.; & Weyers, R. E. (1998). “Modeling the time-to-corrosion cracking in chloride contaminated reinforced concrete structures,” Materials, 95, pp. 675-681.

[7] Chernin L.; Val D. V.; Volokh K. Y. (2010) “Analytical modeling of concrete cover cracking caused by corrosion of reinforcement” Materials and Structures, 43(4), pp. 543-556.

[8] Michel A.; Pease B. J.; Peterová A.; et al. (2014) “ Penetration of corrosion products and corrosion-induced cracking in reinforced mortar: Experimental investigations and numerical simulations” Cement and Concrete Composites, 47, pp. 75-86.

[9] Zhao, Y. X.; Wu, Y. Y.; Jin, W. L. (2013) " Distribution of millscale on corroded steel bars and penetration of steel corrosion products in concrete," Corrosion science, 66, pp. 160-168.
[10] Zhao, Y. X.; Ding, H. J.; Jin, W. L. (2014) "Development of the corrosion-filled paste and corrosion layer at the steel/concrete interface," Corrosion Science, 87, pp. 199–210.
[11] Zhang, X. W. (2021) " Non-uniform distribution of steel corrosion products and corrosion-induced concrete cover cracking, " Zhejiang University. (in Chinese)
[12] Dong J. F. (2018) "Cracking and spalling of reinforced concrete structures under simultaneous loading and chloride penetration," Zhejiang University. (in Chinese)
[13] Wang Y. Z. (2022) "Research on the prediction of corrosion-induced cracking considering corrosion products filling-overflow behavior," Zhejiang University. (in Chinese)
[14] ASTM. (1999) "Standard practice for preparing, cleaning, and evaluating corrosion test specimens," G1-90, West Conshohoken, PA.
[15] CBMF. (2017) "Methods for chemical analysis of cement," GB/T 176-2017, General Administration of Quality Supervision, Inspection and Quarantine of the People's Republic of China; Standardization Administration of the People's Republic of China, Beijing.
[16] Kim, Y. Y.; Lee, K. M.; Bang, J. W.; & Kwon, S. J. (2014) "Effect of W/C ratio on durability and porosity in cement mortar with constant cement amount," Advances in Materials Science and Engineering, 2014. DOI: 10.1155/2014/273460.
[17] Grathwohl, P. (2012) Diffusion in natural porous media: contaminant transport, sorption/desorption and dissolution kinetics (Vol. 1). Springer Science & Business Media, USA.